LA-2310

LOS ALAMOS SCIENTIFIC LABORATORY
OF THE UNIVERSITY OF CALIFORNIA o LOS ALAMOS NEW MEXICO

DOSIMETRY FOR THE GODIVA II CRITICAL ASSEMBLY

NEUTRON FLUX AND TISSUE DOSE MEASUREMENTS

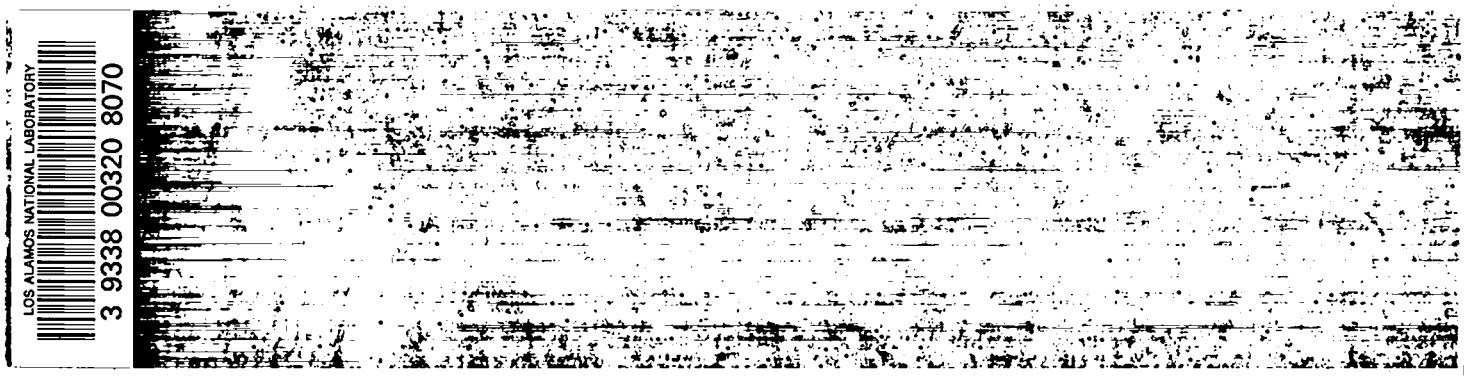

LEGAL NOTICE

Printed in USA. Price $1.25. Available from the

Office of Technical Services
U. S. Department of Commerce
Washington 25, D. C.

LA-2310
INSTRUMENTS
(TID-4500, 14th edition)

LOS ALAMOS SCIENTIFIC LABORATORY
OF THE UNIVERSITY OF CALIFORNIA LOS ALAMOS NEW MEXICO

REPORT WRITTEN: March 1959

REPORT DISTRIBUTED: September 28, 1959

DOSIMETRY FOR THE GODIVA II CRITICAL ASSEMBLY

NEUTRON FLUX AND TISSUE DOSE MEASUREMENTS

by

J. A. Sayeg
E. R. Ballinger, USAF (MC)
P. S. Harris

Contract W-7405-ENG. 36 with the U. S. Atomic Energy Commission

ABSTRACT

Estimates of neutron flux and tissue dose as a function of distance were obtained for the Los Alamos Godiva II critical assembly. Three independent types of measurements were performed: (1) neutron flux by means of the threshold detectors Pu^{239}, Np^{237}, U^{238}, and S^{32}, and bare and cadmium-covered Au^{197} foils; (2) neutron tissue dose by means of the Hurst polyethylene-ethylene proportional counter; and (3) neutron and gamma tissue dose by means of beryllium-shelled tissue-equivalent and graphite-CO_2 ionization chambers. The results for tissue dose as obtained by the above methods showed good agreement.

ACKNOWLEDGMENTS

The authors wish to express their appreciation to the critical assembly Group (N-2) and to Groups P-2, P-4, and H-4 for their assistance in these experiments.

CONTENTS

TABLES

ILLUSTRATIONS

CHAPTER 1

INTRODUCTION

This investigation was performed to provide an estimate of the neutron flux and tissue dose as a function of distance for the Los Alamos Godiva II critical assembly and was initiated to provide a calibration for future biological experiments to be carried out by the Biomedical Research Group (H-4) of this Laboratory.

Three independent types of measurements were carried out. These included:

1. Fast and thermal neutron flux measurements employing the threshold detectors Pu^{239}, Np^{237}, U^{238}, and S^{32}, and bare and cadmium-covered Au^{197} foils.
2. Neutron tissue dose measurements with the Hurst polyethylene-ethylene proportional counter.
3. Neutron and gamma tissue dose measurements with beryllium-shelled tissue-equivalent and graphite-CO_2 ionization chambers.

CHAPTER 2

MATERIALS AND METHODS

2.1 Description of Godiva II Critical Assembly

The Godiva II critical assembly (1,2) is a bare mass of approximately 60 kg of enriched U^{235}. The critical mass is a right circular cylinder 7 in. in diameter (with a spherically shaped top), mounted on a triangular stand (see Fig. 1). The stand houses the electronic control circuitry. The critical mass is surrounded by a wire screen cage 9 in. in diameter. The horizontal midplane of the critical mass is approximately 78-1/2 in. from the concrete Kiva* floor. The Kiva is located 1/4 mile from the control building from which the reactor is operated remotely. Figure 2 shows the placement of Godiva with respect to the Kiva geometry.

*"Kiva" is the Indian name for ceremonial hut and is used for the buildings which house the critical assemblies.

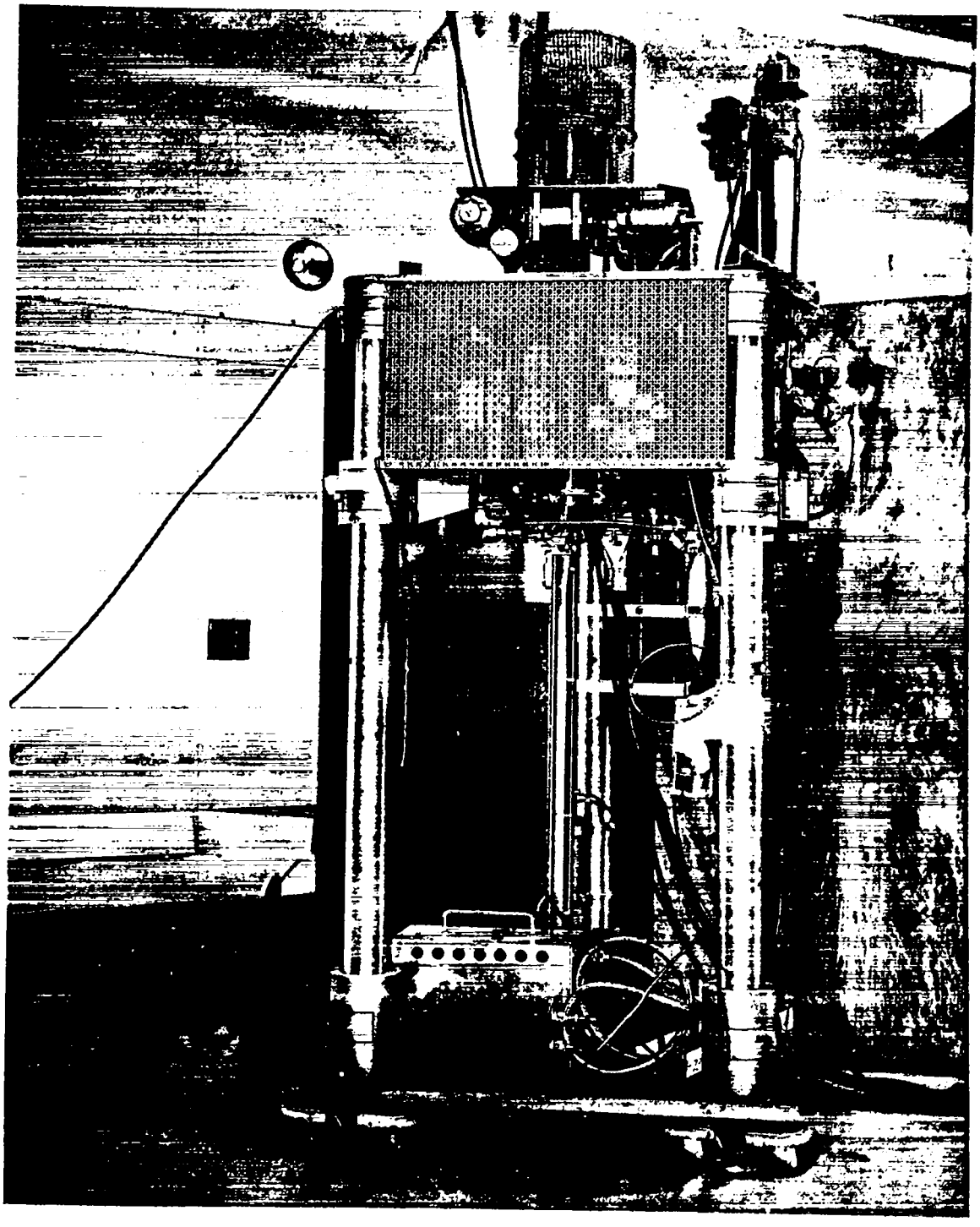

Fig. 1. Godiva II critical assembly mounted on stand.

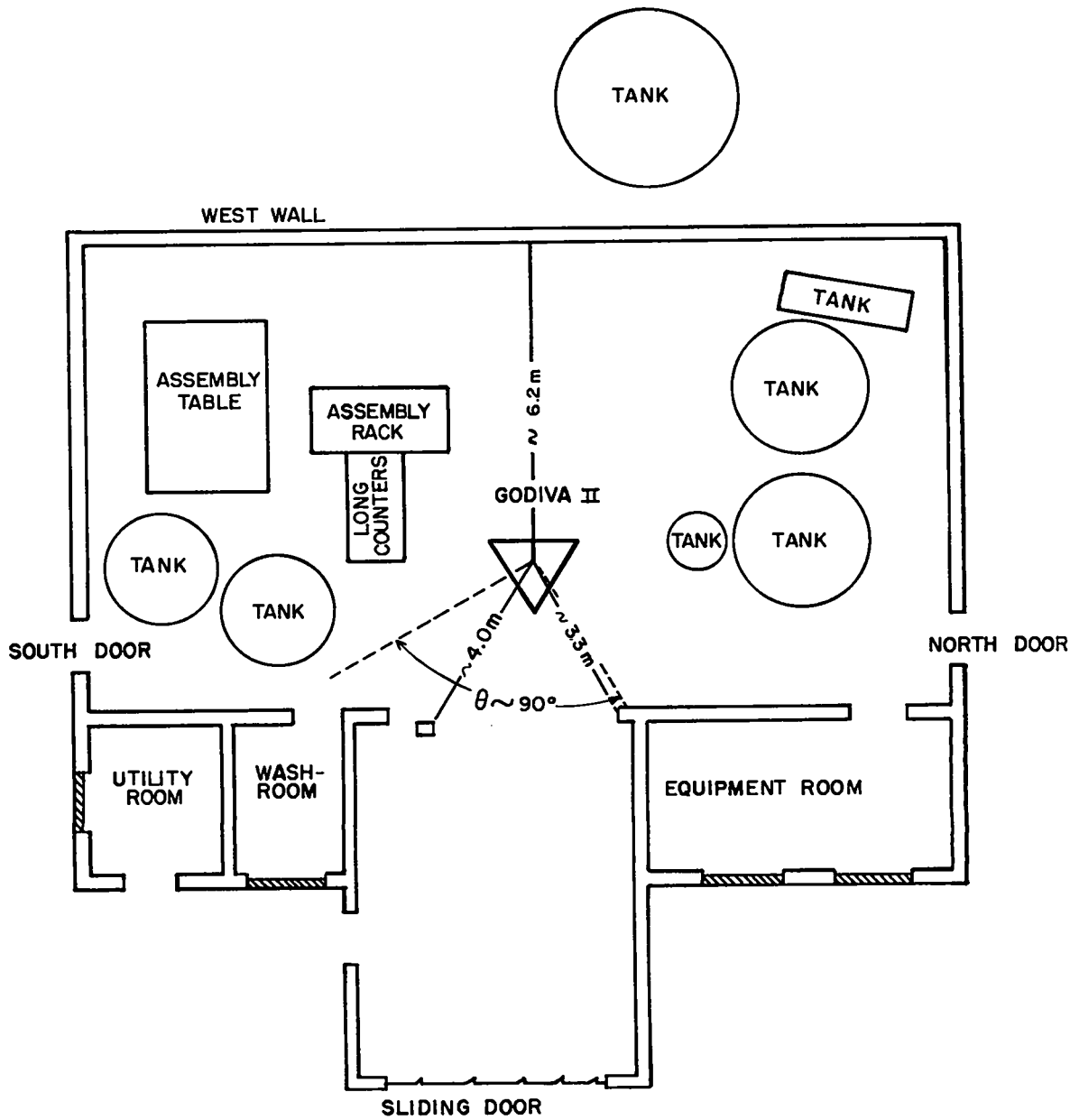

Fig. 2. Godiva placement with respect to Kiva geometry (θ is the quadrant used in the neutron flux and tissue dose determinations).

The assembly can be used for burst irradiations or for power runs. Several instruments and techniques are available for monitoring the irradiations:

1. A thermocouple (for burst irradiations) which measures the temperature rise of the critical mass.

2. An ionization chamber (for steady power experiments) located on the west wall of the Kiva.

3. A U^{235} fission chamber surrounded by cadmium located in the triangular stand approximately 20 in. beneath the critical mass.

4. Sulfur foils.

Since the measured ionization current (as mentioned in item 2 above) is largely dependent on the scattered radiation in the Kiva, the ionization chamber type of monitoring is not suited for accurate monitoring from day to day but rather serves as a rough indicator.

The method which has been used most extensively by our Laboratory personnel is sulfur activation. Sulfur activation gives rise to radioactive phosphorus through the $S^{32}(n,p)P^{32}$ reaction. The activated P^{32} is then counted on a beta plastic scintillation counter (described in Section 2.2.2). This type of monitoring has been used as a primary standard for both bursts and power runs. The disadvantage of the sulfur method for power runs, however, is that it is used in conjunction with the linear amplifier and the exposure can be evaluated only after the radiation has been given

(which prevents any great precision in reproducibility).

The U^{235} cadmium-covered fission counter has been calibrated against the primary sulfur pellet standard to provide more accurate exposures. The following data indicate the geometry and calibration factors to be used:

1. Pellet size: 1-1/2 in. in diameter, 3/8 in. thick.
2. Weight: 20 g.
3. Placement: in aluminum cans at center of the top surface of the protective screen cage.
4. Observed Calibration:

   Burst

   1°C of "peak" temperature rise = 3018 c/m (ICR)* of sulfur pellet.

   Power Run

   17.5 fission counts = 1 c/m (ICR) of sulfur pellet.

2.2 Neutron Flux Measurements

The method of Hurst (3) was followed for the measurement of the fast neutron flux. The threshold detectors Pu^{239}, Np^{237}, U^{238}, and S^{32} were used to measure fast neutron fluxes above the following threshold energies:

---

*(ICR) is the initial counting rate of the foil detector.

Pu^{239} (surrounded by 2 cm of B^{10}), >4 kev

Np^{237}, >0.75 Mev

U^{238}, >1.5 Mev

S^{32}, >2.5 Mev

To facilitate handling for irradiation, all foils were surrounded by cadmium and placed in spheres containing 2 cm of B^{10}. The fission foils of Pu^{239}, Np^{237}, and U^{238} were approximately 1/2 in. in diameter and varied in mass from 0.05 to 3.5 g.

2.2.1 Fission Gamma Scintillation Counter

The fission foils were counted on a 1-1/2 in. diameter, 1-1/2 in. thick thallium-activated sodium iodide crystal mounted on an RCA 6655 phototube (see Fig. 3). A 1/4 in. thick lead absorber was interposed between the foil and crystal to reduce the natural background of the foils (especially that of Np^{237}, which exhibited the largest natural background). The output of the phototube was connected to a Model 250N preamplifier, thence to a Model 250 amplifier, a Model 120 dual-channel analyzer, and two Model 775 scalers. These electronic components provided a means of counting simultaneously at two different bias values.

Calibration of the counting system was achieved in the following manner. The relation of gamma ray energy to

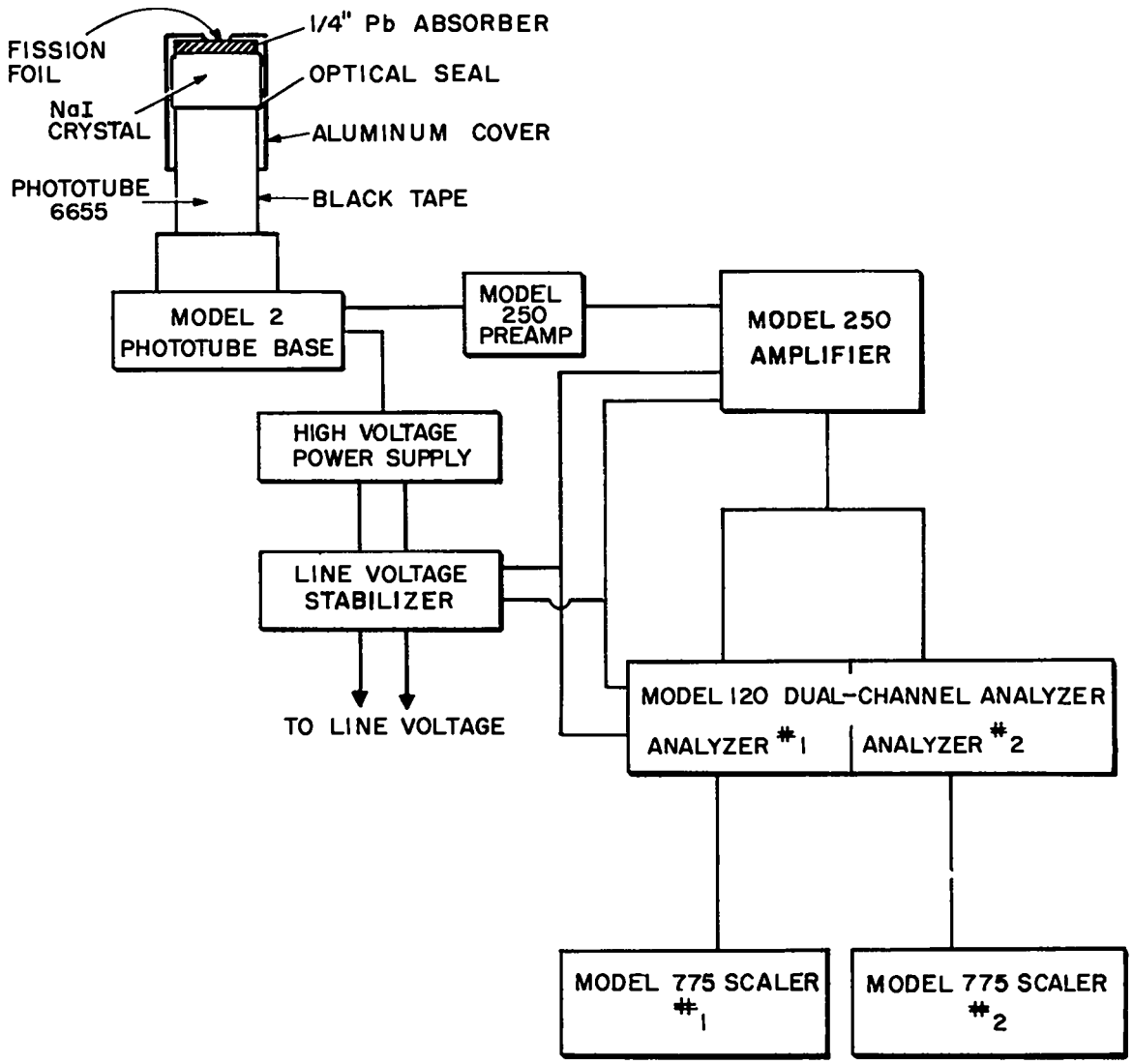

Fig. 3. Block diagram of fission foil counting system.

counter bias was obtained by counting Na^{22} and Cs^{137} samples in 1 volt channel widths. These samples provided gamma ray energies of 0.51, 0.66, and 1.28 Mev. The natural background of the Np^{237} sample exhibited a strong photopeak at 0.31 Mev and served as an additional check (see Fig. 4). The threshold counting bias values were arbitrarily chosen at 0.51 and 1.10 Mev. The Na^{22} sample was used as a standard source to check any drift in gain of the counting equipment. Calibration of the counting system at the two bias values was achieved by irradiating a thin (1 mil, 0.047 g) Pu^{239} foil in the Los Alamos Water Boiler thermal column. The Water Boiler flux was checked by comparison of bare and cadmium-covered gold foils irradiated in the Los Alamos Standard Pile (4). The calibration constant K for Pu^{239} was evaluated from the relation

$$K_{t,b} = \frac{F_t}{(A_{t,b}/m) \times f} \times \frac{\sigma(\text{thermal})}{\sigma(\text{fast})} \qquad (1)$$

where

$K_{t,b}$ = calibration constant for time t and bias value b

F_t = integrated thermal neutron flux, n/cm^2

$A_{t,b}$ = observed Pu^{239} activity at time t and bias b

m = mass of irradiated foil, g

f = self-shielding and flux depression factor for a foil of finite thickness (5)

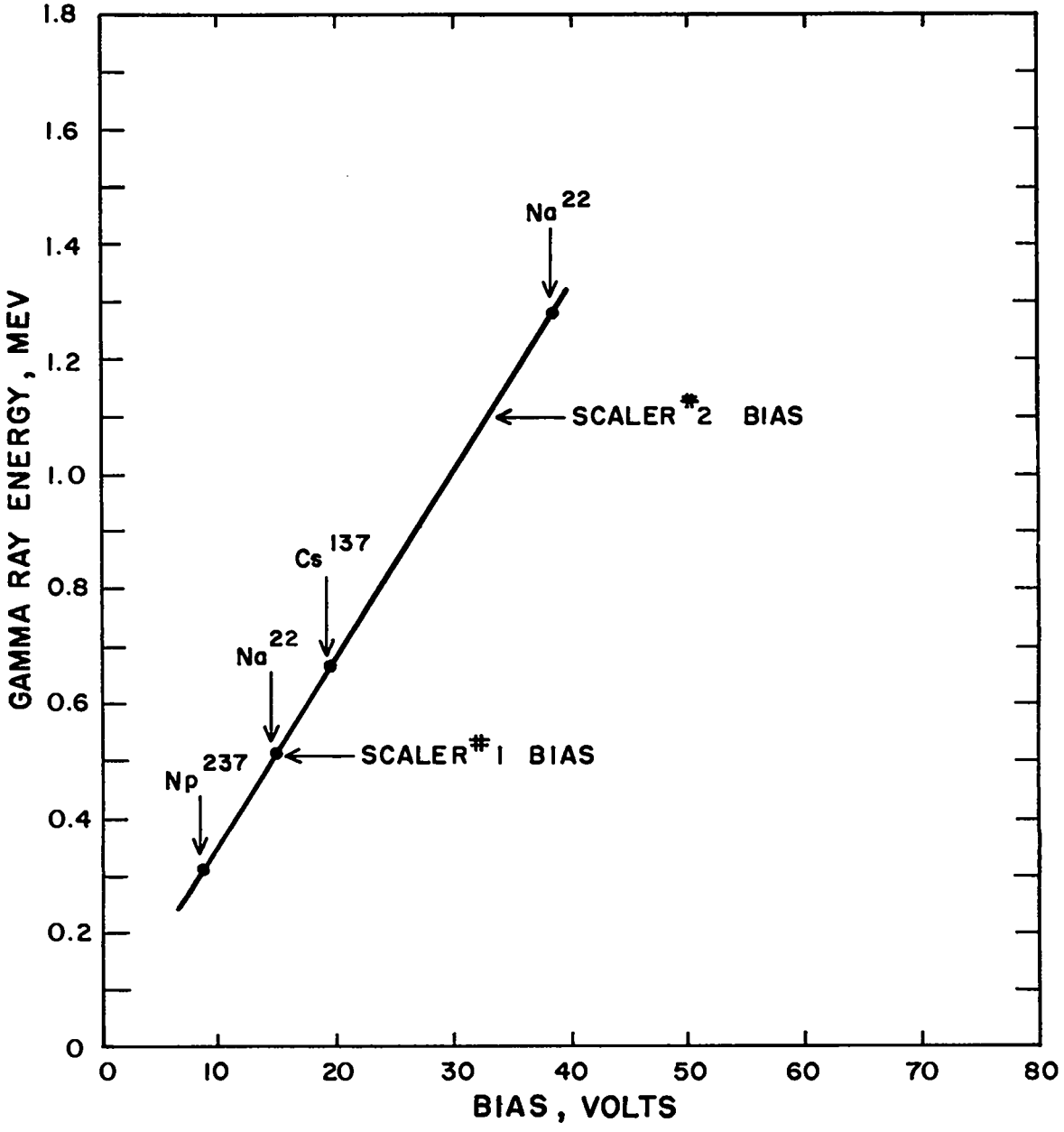

Fig. 4. The relation of gamma ray energy to counter bias.

σ(thermal) = fission cross section for thermal neutrons, barns

σ(fast) = fission cross section for fast neutrons, barns

The irradiation data for the thermal neutron calibration were as follows:

1. Pu^{239} foil number: 49-1-1.
2. Foil mass: 0.047 g.
3. Water Boiler geometry: south thermal column, port No. 1, 40-1/8 in. from the bismuth wall.
4. Activation (2200 meter) flux: 9.47×10^{7} $n/cm^2/sec/kw$ (10 per cent accuracy).
5. Exposure: 1 kw for 3 min (starting time taken at 1/3 power to compensate for exponential build-up of flux).
6. Total integrated flux, F_t: 1.70×10^{10} n/cm^2.

Observations under these conditions gave the following results:

1. Activity at 2 hr and 0.51 Mev bias, $A_{2,0.51}$, was 71,280 c/m.
2. Activity at 2 hr and 1.1 Mev bias, $A_{2,1.1}$, was 16,200 c/m.

Hence

$$K_{2,0.51} = \frac{1.70 \times 10^{10} \text{ n/cm}^2}{\left[(71{,}280 \text{ c/m})/0.047 \text{ g}\right] \times 1.18} \times \frac{774}{2}$$

$$= 3.68 \times 10^{6} \frac{\text{n/cm}^2}{\text{c/m/g}} \qquad (2)$$

Likewise

$$K_{2,1.1} = 1.62 \times 10^7 \frac{n/cm^2}{c/m/g} \quad (3)$$

The calibration constants for Np^{237} and U^{238} were calculated from the expressions

$$K_{Np} = \frac{\sigma_{Pu}}{\sigma_{Np}} \times K_{Pu} \quad (4)$$

and

$$K_{U} = \frac{\sigma_{Pu}}{\sigma_{U}} \times K_{Pu} \quad (5)$$

and are tabulated in Table I for the two bias values used. Also tabulated in Table I are the natural background values of the fission neutron detectors.

2.2.2 Sulfur Pellet Beta Counter

A 2 in. diameter, 5/32 in. thick plastic scintillator, covered by 2 mils of aluminum foil and connected to an RCA 6655 phototube, was used to measure the induced P^{32} beta activity in the sulfur pellet discs. The applied voltage to the phototube was 1000 volts. Two sizes of sulfur pellets were used:

1. A 0.44 in. diameter, approximately 0.15 in. thick pellet, which was placed inside the B^{10} sphere.
2. A 1-1/2 in. diameter, 3/8 in. thick pellet, which was used in free air.

Counting efficiency for the 1-1/2 in. diameter pellet

TABLE I

CALIBRATION CONSTANTS AND NATURAL BACKGROUND OF THE FISSION NEUTRON DETECTORS Pu^{239}, Np^{237}, AND U^{238} WITH THE SINGLE TUBE FISSION GAMMA COUNTER

	Counter Calibration Constant K,[a] $n/cm^2/c/m/g$			Natural Background of Fission Foils, c/m/g		
	K_{Pu}	K_{Np}	K_U	Pu^{239}	Np^{237}	U^{238}
0.51 Mev counter energy bias (natural counter background 99 c/m)	3.68×10^6	4.89×10^6[b]	1.36×10^7	3115	52,130	591
1.1 Mev counter energy bias (natural counter background 36 c/m)	1.62×10^7	2.15×10^7	5.99×10^7	173	0	38

(a) Values of the fission cross sections used in calculations: σ_{Pu}(thermal) = 774 barns; σ_{Pu}(fast) = 2.0 barns; σ_{Np}(fast) = 1.5 barns; and σ_U(fast) = 0.54 barn.

(b) The Np^{237} calibration constant at the lower bias can be used only when there is a negligible amount of epithermal neutrons. The epithermal neutrons penetrating the cadmium cover inside the B^{10} sphere give rise to a 2.1 day contaminant activity due to the $Np^{237}(n,\gamma)Np^{238}$ reaction.

was approximately 10 times that of the smaller pellet, and when the larger pellet was burned and counted [according to the method described by Reinhardt and Davis (6)], the sensitivity was increased by a factor of approximately 15, or a final sensitivity of roughly 150 times that of the small pellet. The counter was calibrated by exposing standard pellets to 14 Mev neutrons from the Los Alamos Cockcroft-Walton accelerator. The discs were placed a minimum distance of 10 cm from the target-source (in the 90° plane).

The effective cross section for a fission spectrum was calculated to be 0.230 barn for an effective threshold of 2.5 Mev. The 14 Mev cross section was taken as 0.248 barn (7). The calibration constants K_s are shown in Table II.

TABLE II

CALIBRATION CONSTANTS OF THE SULFUR BETA COUNTER FOR NEUTRON FLUX GREATER THAN 2.5 MEV

Sulfur Pellet Type	K_s, $\frac{n/cm^2}{c/m\ (ICR)}$
Small	1.05×10^8
Small "burnt"	2.90×10^7
Large	9.87×10^6
Large "burnt"	6.88×10^5

2.2.3 Gold Gamma Scintillation Counter

The gold counter consisted of a 1-1/2 in. diameter, 1-1/2 in. thick sodium iodide crystal with a 1/16 in. (approximately 400 mg/cm^2) aluminum absorber between the crystal and foil to be counted. This absorber was used to eliminate the beta ray activity emitted by Au^{198}. The counter was biased at approximately 0.03 Mev, where a counting plateau was found. The counting system was calibrated against the Los Alamos Standard Pile by placing a 1/2 in. diameter, 10 mil thick Au^{197} foil in slot No. 10 of the pile. The 2200 meter thermal flux in this position was measured by absolute gold counting and was found to be 2.41 x 10^3 n/cm^2/sec with an accuracy of 10 per cent (8). Cadmium-covered Au^{197} foils indicated the cadmium ratio to be about 30. The calibration foils were exposed for approximately 2-1/2 half-lives (approximately 7 days). The gold counter calibration constant K_g was evaluated by the formula*

$$K_g = \frac{F_s}{(A/W)/(1 - e^{-\lambda\tau})} \times \frac{1}{\lambda} = 1.34 \times 10^5 \frac{n/cm^2}{c/m/g\ [(ICR)/g]} \quad (6)$$

*Formula derived on basis that $\lambda \times \tau$ (thermal column) is small.

where

F_s = neutron flux (2.41×10^3 n/cm^2/sec)

A = initial counting rate (corrected for the cadmium ratio)

W = weight of foil (0.66 g)

λ = decay constant for Au^{198} (2.97×10^{-6}/sec)

τ = time of exposure at the Standard Pile

A Cs^{137} source was used as a standard to check any change in gain of the counting system.

2.3 Neutron Tissue Dose Measurements with the Hurst Polyethylene-Ethylene Proportional Counter

A Hurst proportional counter, with a polyethylene wall and ethylene gas (9,10), was used. The counter was used as a flow counter and connected to a voltage divider which placed 0.285 of the collecting voltage on the field tubes. The voltage applied to the central wire was +2250 volts. The output of the counter was connected to a 130N line-driving preamplifier, a 101A linear amplifier with delay line clipping, and finally to a 100-channel analyzer. Alpha calibration curves were taken before and after the Godiva experiments.

The absorbed dose in ethylene D_{eth} was evaluated from the formula

$$D_{eth} = 1.602 \times 10^{-8} \frac{E_\alpha}{M_{eth}} \times \frac{A_g}{A_\alpha} \qquad (7)$$

where

1.602×10^{-8} = conversion factor from Mev/g to rads

E_α = energy of calibrating Pu^{239} alpha source (5.14 Mev)

M_{eth} = mass of ethylene gas in sensitive volume (0.0734 g at STP)

A_g = area representing the dose delivered by the Godiva neutrons

A_α = area representing the dose delivered by the calibrating alpha source

and was normalized to the ICR of the sulfur monitor. Figure 5 shows representative integral bias curves.

The dose in tissue D_T was calculated from the expression

$$D_T = \frac{D_{eth}}{1.45 \pm 0.15} \tag{8}$$

where the factor 1.45 ± 0.15 is the ratio of first collision doses in ethylene and tissue, respectively (9).

2.4 Tissue Dose Measurements with the Tissue-equivalent and Graphite-CO_2 Ionization Chambers

The method employing tissue-equivalent and graphite-CO_2 ionization chambers, described by Rossi and Failla (11), was used in the neutron and gamma tissue dose evaluations. The ionization chambers used, their performance data, and the formulation of evaluation have been discussed in detail in Ref. 5. A brief review, however, has been included.

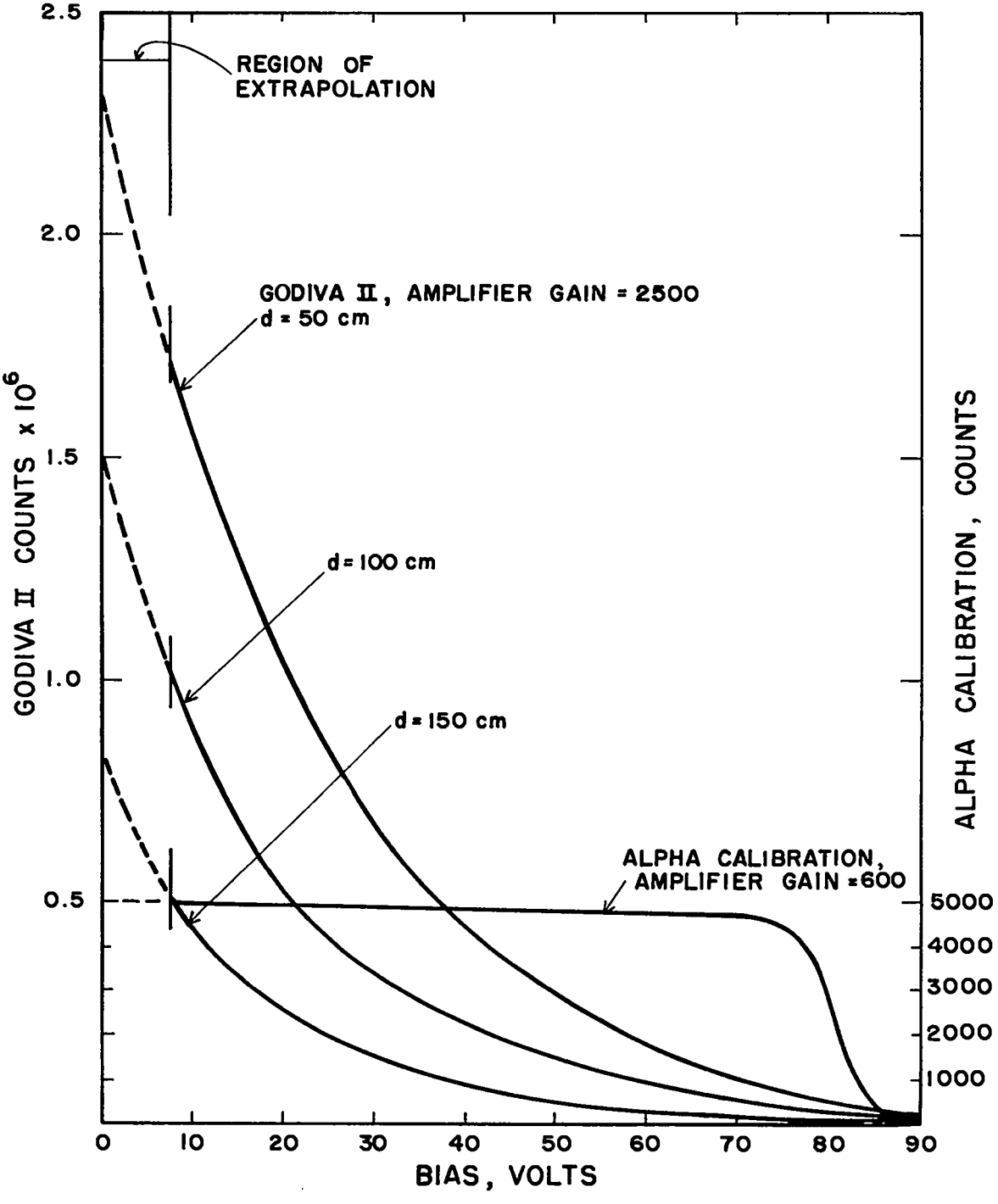

Fig. 5. Integral bias curves with the Hurst proportional counter.

Figures 6 and 7 show a schematic and a photograph of a condenser-type tissue-equivalent ionization chamber. The chamber is approximately 1-3/8 in. in diameter and 6-1/2 in. long. The outer shell is constructed of beryllium to ensure a low thermal neutron activation of chamber components, good conductivity, and gas tightness. The capacitance is approximately 50 μμfd, dependent on the dielectric employed (i.e., Teflon or polystyrene). The head portion contains the sensitive volume of approximately 7 cm^3, wall liner thickness of 1/8 in. (340 mg/cm^2), and center electrode of 3/8 in. diameter. Liners and center electrodes of different materials can be placed in the head, thus satisfying conditions for various types of dose measurements. The stem is composed of dielectric and a beryllium center tube which permits gas filling from the rear portion of the chamber. The chamber wall liner was operated at +600 volts with respect to the center electrode.

The chambers were used in conjunction with a specially designed charger-reader slideback voltmeter unit, a schematic of which is shown in Fig. 8. The unit employed a Victoreen 5803 subminiature tube in a slideback circuit. This instrument can be used as a current-indicating or -integrating device, by changing from a resistor to a condenser circuit. It is able to measure both plus and minus polarity with a precision of 1 per cent.

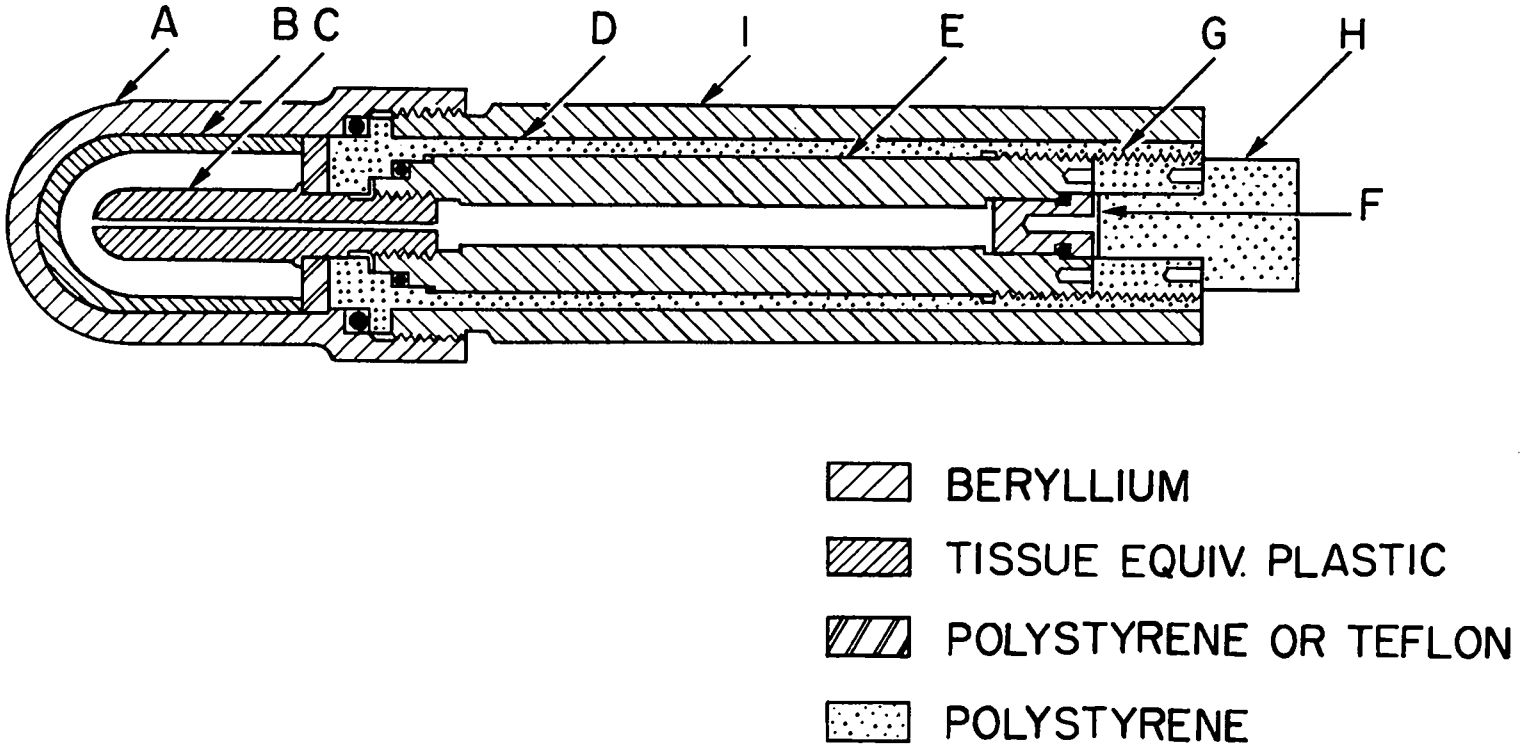

Fig. 6. Schematic of condenser-type tissue-equivalent ionization chamber: A, beryllium head shell; B, chamber wall liner; C, chamber center electrode; D, polystyrene dielectric; E, beryllium center stem conductor; F, filling plug; G, polystyrene cap; H, polystyrene plug; and I, beryllium stem shell.

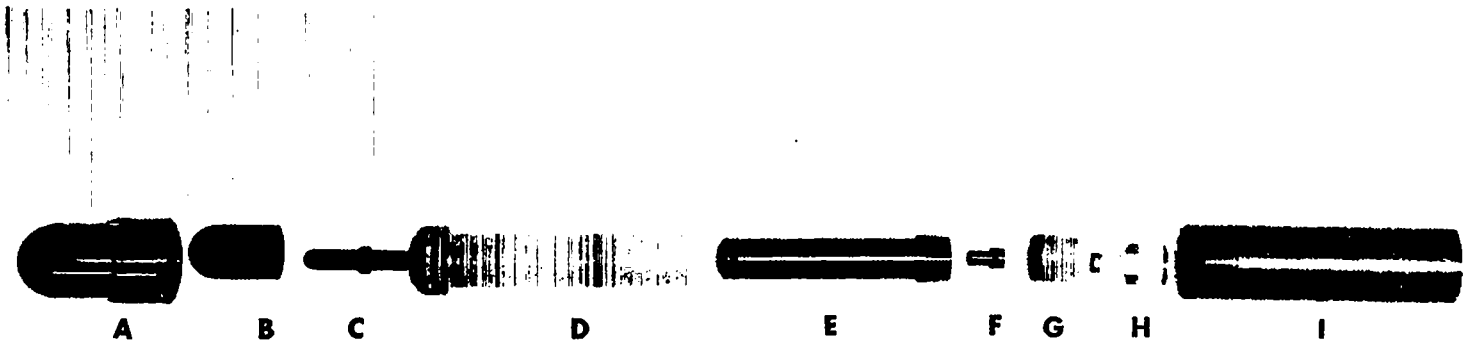

Fig. 7. Photograph of condenser-type tissue-equivalent ionization chamber (see Fig. 6 for code).

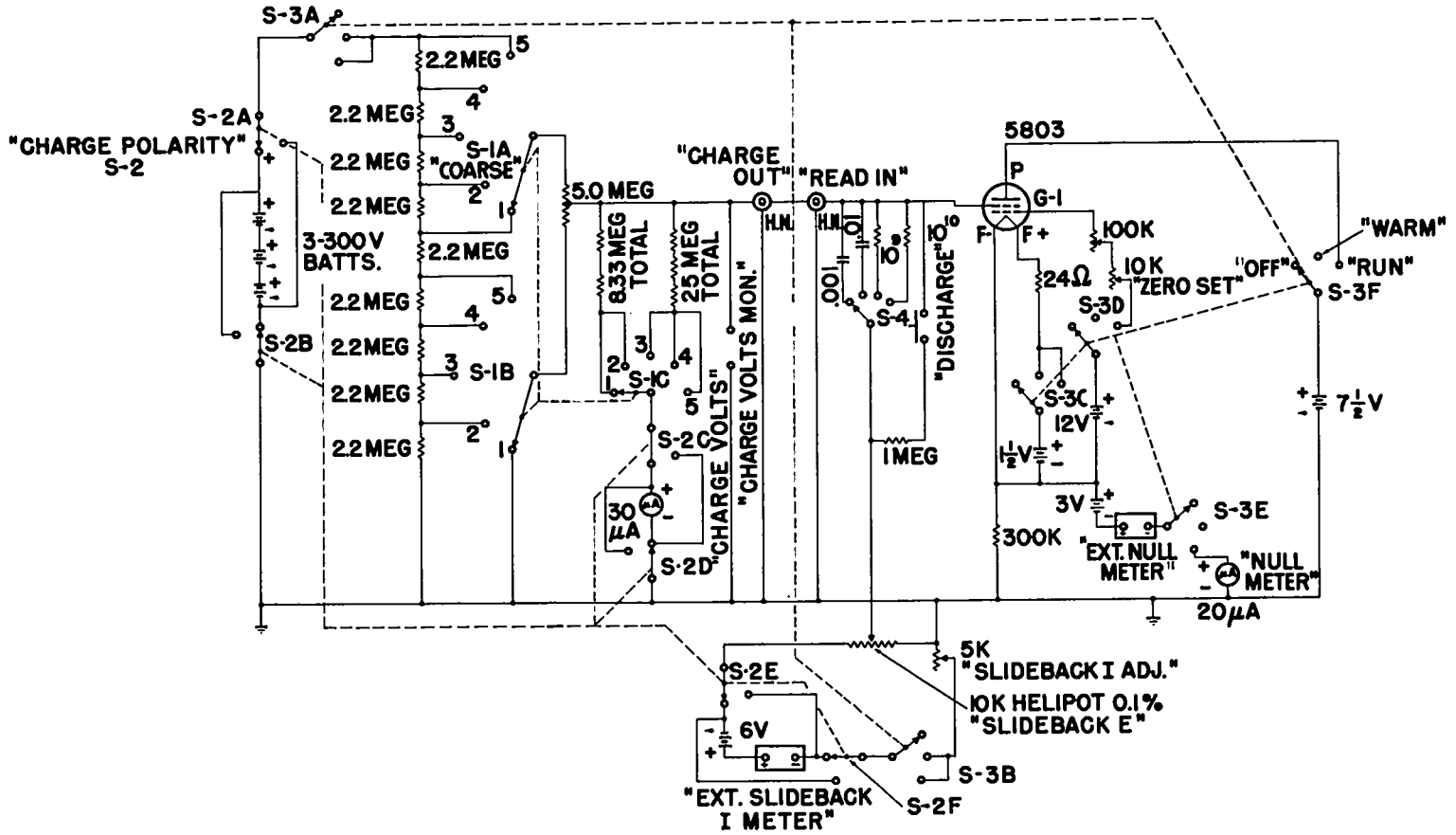

Fig. 8. Schematic diagram of charger-reader slideback voltmeter unit.

The equations used in the neutron and gamma tissue dose evaluations were

$$T = aN + b\gamma \tag{9}$$

$$G = kN + b\gamma \tag{10}$$

whence

$$N = \frac{T - G}{a - k} \tag{11}$$

and

$$\gamma = G - kN \tag{12}$$

where

T = response of tissue-equivalent ionization chamber in terms of a hard X-ray or gamma-ray calibration, roentgens

G = response of the graphite-CO_2 ionization chamber in terms of a hard X-ray or gamma-ray calibration, roentgens

N = neutron tissue dose, rads

γ = gamma tissue dose, rads

a = efficiency of neutron dose measurement, roentgens per tissue rad

k = neutron response of the graphite-CO_2 chamber, roentgens per tissue rad

The values of a and k were estimated from first collision theory and were found to be 1.03 and 0.12 roentgens per tissue rad, respectively, for a fission spectrum. The coefficient b represents the roentgen-to-rad conversion factor and is equal to 1.03 roentgens per tissue rad.

CHAPTER 3

RESULTS

3.1 Measurement of Neutron Flux

The results obtained with the threshold detectors Pu^{239}, Np^{237}, U^{238}, and S^{32} are shown in Table III as a function of distance from the center of the assembly. In Table IV is shown the breakdown of the measured fluxes into their respective energy intervals. In Table V are shown the flux ratios as a function of distance.

Both bursts and short power runs (approximately 5 min duration) were evaluated with no significant difference in results. It is seen that an approximate inverse-square relation is followed from 15 to 200 cm. The fall-off for distances greater than 200 cm is less than inverse square and is due to room scattering. The data between 35 and 200 cm* are best represented by the least-squares equations

*The 15.8 and 17.0 cm data were not used in the least-squares analysis because errors in positioning of these close points with respect to the rather large source contributed a large proportion of the total error in the analysis.

TABLE III

FAST NEUTRON FLUX[(a)] AS MEASURED WITH THE THRESHOLD DETECTORS Pu^{239}, Np^{237}, U^{238}, AND S^{32} AT THE GODIVA II CRITICAL ASSEMBLY

Distance from Center (horizontal midplane), cm	Flux, $(n/cm^2 \times 10^9)$/°C of burst[(b)]			
	$E_n > 0.004$ Mev	$E_n > 0.75$ Mev	$E_n > 1.5$ Mev	$E_n > 2.5$ Mev
	Pu^{239}	Np^{237}	U^{238}	S^{32}[(c)]
15.8	99.5	83.0	43.8	15.3
17.0	83.2	72.6	35.2	13.8
35.0	15.7	14.4	7.17	2.65
50.0	8.55	7.84	3.73	1.44
75.0	3.72	3.44	1.56	0.544
100[(d)]	2.22	1.83	0.870	0.357
150	0.965	0.779	0.376	0.141
200	0.606	0.450	0.218	0.0685
250	0.542	0.438	0.175	0.0363

(a) All foils were placed in 2 cm B^{10} spheres.

(b) Temperature corresponds to peak temperature rise of exposure.

(c) Sulfur pellets placed outside the B^{10} sphere exhibited a flux which was approximately 20 per cent higher.

(d) Shadow cone measurements taken at 100 cm indicated the scattered flux background to be approximately 7 per cent for Pu^{239}, 6 per cent for Np^{237}, and 5 per cent for U^{238}.

TABLE IV

FLUX DETERMINATIONS[a] WITH THRESHOLD DETECTORS AT THE GODIVA II CRITICAL ASSEMBLY

Threshold Detector Type	Measured Energy Interval, Mev	Flux, $(n/cm^2 \times 10^9)/°C$ of burst[b]	Per cent of Neutrons in Energy Interval
Pu-Np	0.004 - 0.75	0.39	17.6
Np-U	0.75 - 1.5	0.96	43.2
U-S	1.5 - 2.5	0.51	23.0
S	>2.5	0.36	16.2

(a) For a distance of 100 cm from the center of the source (in the horizontal midplane).

(b) Temperature rise corresponds to peak temperature rise of burst.

TABLE V

RATIO OF MEASURED FLUXES AT THE GODIVA II CRITICAL ASSEMBLY

Distance to Center of Godiva II (horizontal midplane), cm	Threshold Detector Measurements			Expected Ratios from Rosen's Data (Ref. 12)		
	F_{Np}/F_{Pu}	F_U/F_{Pu}	F_S/F_{Pu}	F_{Np}/F_{Pu}	F_U/F_{Pu}	F_S/F_{Pu}
15.8	0.834	0.440	0.154			
17.0	0.872	0.423	0.166			
35.0	0.917	0.457	0.169			
50.0	0.917	0.436	0.168			
75.0	0.925	0.419	0.205			
100	0.824	0.392	0.161	0.571	0.330	0.182
150	0.807	0.390	0.146			
200	0.743	0.360	0.113			
250	0.808	0.402	0.067			

For E_n > 0.004 Mev

$$F_{Pu} = 2.24 \times 10^{13}\ d^{-2.01} \quad (13)$$

For E_n > 0.75 Mev

$$F_{Np} = 1.91 \times 10^{13}\ d^{-2.01} \quad (14)$$

For E_n > 1.5 Mev

$$F_{U} = 0.93 \times 10^{13}\ d^{-2.01} \quad (15)$$

For E_n > 2.5 Mev

$$F_{S} = 0.34 \times 10^{13}\ d^{-2.01} \quad (16)$$

where F is the neutron flux generated per degree of peak temperature rise of burst for the detector in question, and d is the distance in centimeters from the center of the assembly (in horizontal midplane).

It will be noted that the common slope (-2.01 $\pm$ 0.01) has been used. The slopes of individual regression lines tend to become steeper as threshold energy increases (even though they are not significantly different in the strict statistical sense). These slopes are -1.90 $\pm$ 0.02 at a threshold of 0.004 Mev, -2.02 $\pm$ 0.01 at 0.75 Mev, -2.03 $\pm$ 0.01 at 1.5 Mev, and -2.09 $\pm$ 0.03 at 2.5 Mev. These results indicate that enough scattering has occurred (probably in the B^{10} ball itself) between the source and the detector to cause the deviation from the expected inverse-square relation.

An attempt was made to correlate the flux ratios with the spectral measurements of Rosen (12) with Godiva I. The results, however, showed a large disagreement (see Table V).

Both the Np^{237}/Pu^{239} and U^{238}/Pu^{239} flux ratios were high and seemed to indicate a perturbation by the B^{10} ball in which the foils were placed. The disagreement in the ratios developed between the nuclear track plate data of Rosen and the fission foil data is apparently due to two factors. These are: (1) the values of the effective thresholds and cross sections for the fission foils in the experimental arrangement used; and (2) the rate of change of neutron flux per unit energy interval over the region where the fission threshold is changing. Studies are now underway at Oak Ridge (13) to determine by Monte Carlo calculations the magnitude of the B^{10} perturbation.

The thermal neutron flux was estimated by exposing bare and cadmium-covered gold foils. The relation of flux to distance is shown in Table VI with the cadmium fraction.

The first collision neutron tissue dose was calculated from the formula

$$\begin{aligned} D_n = {} & 0.93 \times 10^{-9} \frac{\text{rad}}{\text{n/cm}^2} \times (F_{Pu} - F_{Np}) \text{ n/cm}^2 \\ & + 2.33 \times 10^{-9} \frac{\text{rad}}{\text{n/cm}^2} \times (F_{Np} - F_U) \text{ n/cm}^2 \\ & + 2.98 \times 10^{-9} \frac{\text{rad}}{\text{n/cm}^2} \times (F_U - F_S) \text{ n/cm}^2 \\ & + 3.63 \times 10^{-9} \frac{\text{rad}}{\text{n/cm}^2} \times (F_S) \text{ n/cm}^2 \end{aligned} \qquad (17)$$

TABLE VI

THERMAL FLUX AS MEASURED WITH CADMIUM-COVERED AND BARE GOLD FOILS AT THE GODIVA II CRITICAL ASSEMBLY

Distance from Center (horizontal midplane), cm	Thermal Flux (E_n < 0.5 ev), ($n/cm^2 \times 10^7$)/°C of burst[(a)]	Cadmium Fraction[(b)]
17	1.30	0.13
35	3.92	0.74
75	4.59	1.6
100	4.83	1.8
150	5.44	2.0
250	5.32	2.2

(a) Temperature corresponds to peak temperature rise of exposure.

(b) Defined as [(bare activity/cadmium-covered activity) - 1]. All measurements were made with 10 mil thick gold foils.

The coefficients before the flux parentheses represent the average first collision tissue dose per neutron per square centimeter for the energy interval under consideration. Table VII (column 2) shows the calculated values normalized to the sulfur pellet monitor. The fast neutron tissue dose per monitor counting rate versus distance from the center of the assembly is best represented by the least-squares fit

$$\frac{\text{tissue rad}}{\text{sulfur monitor (ICR)}} = 19.8\ d^{-2.01 \pm 0.01} \qquad (18)$$

where d is the distance in centimeters from the center of the assembly (horizontal midplane).

The thermal neutron flux was converted to tissue dose for a small biological object the size of a mouse by using the conversion factor 5×10^{-11} rad/n/cm^2. However, the thermal neutron tissue dose represented less than 0.2 per cent of the fast neutron tissue dose and was neglected in the total dose evaluations.

3.2 Measurement of Neutron Tissue Dose with the Hurst Polyethylene-Ethylene Proportional Counter

Table VII (column 3) shows the results obtained in tissue with the Hurst proportional counter. Only four distances (50, 100, 150, and 200 cm) were investigated. The tissue dose data between 50 and 200 cm are best represented

TABLE VII

NEUTRON AND GAMMA TISSUE DOSES AS A FUNCTION OF DISTANCE FOR THE GODIVA II CRITICAL ASSEMBLY[a]

Distance from Center (horizontal midplane), cm	Neutron Tissue Dose			Gamma Tissue Dose
	Threshold Detectors	Hurst Proportional Counter	Tissue-equivalent Ionization Chamber	Graphite-CO_2 Ionization Chamber
15.8	8.29×10^{-2}			
17.0	7.08×10^{-2}			
35.0	1.43×10^{-2}			
50.0	7.44×10^{-3}	7.22×10^{-3}	6.97×10^{-3}	6.31×10^{-4}
75.0	3.24×10^{-3}			
100	1.80×10^{-3}	1.91×10^{-3}	1.78×10^{-3}	1.55×10^{-4}
150	7.75×10^{-4}	9.30×10^{-4}	8.11×10^{-4}	9.01×10^{-5}
200	4.69×10^{-4}	5.50×10^{-4}		
250	4.14×10^{-4}			

(a) Normalized to the ICR of the sulfur pellet monitor (see Section 2.1 for conversion constants).

by the least-squares equation

$$\frac{\text{tissue rad}}{\text{sulfur monitor (ICR)}} = 9.87\ d^{-1.85 \pm 0.04} \qquad (19)$$

3.3 Measurement of Neutron and Gamma Tissue Dose by the Tissue-equivalent Ionization Chamber Method

Table VII (column 4) shows the results obtained with the tissue-equivalent and graphite-CO_2 ionization chambers. Only three distances were investigated (50, 100, and 150 cm). The data for neutron dose between 50 and 150 cm are best represented by the least-squares equation

$$\frac{\text{tissue rad}}{\text{sulfur monitor (ICR)}} = 14.9\ d^{-1.96 \pm 0.01} \qquad (20)$$

The gamma dose as evaluated by the graphite-CO_2 chamber represented only a lower limit and was found to be approximately 10 per cent of the neutron dose for the Kiva conditions* under which these experiments were performed.

---

*Because of the numerous experiments which are being carried on in the Kiva assembly buildings, equipment is continually being installed and removed. This constant conveyance of scattering material prevents any constant gamma dose being present in the area.

3.4 Comparative Neutron Dosimetry

The difference between the different experimental systems in the measurement of neutron tissue dose was not significant. A composite analysis, including data from all three systems between 35 and 200 cm, indicated a least-squares fit of

$$\frac{\text{tissue rad}}{\text{sulfur monitor (ICR)}} = 14.8\ d^{-1.95 \pm 0.05} \qquad (21)$$

CHAPTER 4

ACCURACY OF MEASUREMENTS

4.1 Neutron Flux and Tissue Dose by the Threshold Detector Technique

The accuracy of the threshold detector system for measurement of fast neutron flux is almost entirely dependent on the accuracy of the thermal neutron flux calibration and the uncertainties of the quoted fast and thermal neutron cross sections. The estimated accuracy given by the Los Alamos Water Boiler and Standard Pile personnel is 10 per cent for their measured fluxes (8). The quoted fast and thermal neutron cross sections are believed to be uncertain by approximately 10 per cent. Another consideration is the perturbation of the "free air" flux by the B^{10} balls. At present, no accurate estimates of the error are available; however, Monte Carlo calculations are being completed by the Oak Ridge group (13). Hence, at present, it is estimated that this type of measurement has an

uncertainty of approximately 15 per cent.

The accuracy of tissue dose as measured by the threshold detectors is dependent on the following two factors:

1. The uncertainty of the fast neutron flux.
2. The precision of the first collision dose values used to weight the measured spectrum.

Item 1 has been discussed above. Item 2 is mainly dependent on the measured elastic scattering cross sections used in the first collision dose calculations. It is estimated that these measurements contribute an uncertainty of no more than 10 per cent for energies included in the fission spectrum. Hence, a total uncertainty of approximately 18 per cent is ascribed for measurement of tissue dose by this method.

4.2 Proportional Counter Measurements of Radiation Dose

The main uncertainties in this type of measurement include:

1. Extrapolation of the integral bias curve to zero bias.
2. The conversion dose factor which relates the dose measured in the medium in question to that of ethylene.

The uncertainty in the bias extrapolation is believed to be approximately 10 per cent. The uncertainty for the dose conversion factor again depends on the precision of

the measured elastic cross sections. Hurst (9) has estimated the uncertainty for tissue dose conversions to be 1.45 ± 0.15, or approximately 10 per cent. Hence, the total uncertainty is approximately 15 per cent.

4.3 Tissue-equivalent Ionization Chamber Measurements

The accuracy of the measured neutron tissue dose is mainly dependent on:

1. The precision of the X-ray calibration.
2. The neutron response of the graphite-CO_2 chamber [see Equation (10)].

It is thought that the uncertainty of the X-ray calibration is at most 5 per cent. The neutron response factor k, which may have an uncertainty of as much as 50 per cent, contributes an uncertainty of no more than 5 per cent in the neutron dose for the gamma-to-neutron ratios observed (1:10). Hence, a total uncertainty of approximately 10 per cent is assumed.

REFERENCES

1. Wimett, T. F., and J. D. Orndoff, "Applications of Godiva II Neutron Pulses," Second International Conference on Peaceful Uses of Atomic Energy, Geneva, Paper P/419 (August 1958).
2. Radiation Effects Section, "Godiva II, Its Availability and Suitability for Radiation Effects Tests," Sandia Corporation informal report (June 13, 1958).
3. Hurst, G. S., J. A. Harter, P. N. Hensley, W. A. Mills, M. Slater, and P. W. Reinhardt, "Techniques of Measuring Neutron Spectra with Threshold Detectors -- Tissue Dose Determinations," Rev. Sci. Instr. 27, 153 (1956).
4. Graves, A. C., and D. K. Froman, Miscellaneous Physical and Chemical Techniques at the Los Alamos Project, National Nuclear Energy Series, Div. V, Vol. 3, pp. 98-101 (New York: McGraw-Hill Book Company, 1952).
5. Sayeg, J. A., J. H. Larkins, and P. S. Harris, "Experimental Determination of Fast- and Thermal-neutron Tissue Dose," Los Alamos Scientific Laboratory Report LA-2174 (May 28, 1958).

6. Reinhardt, P. W., and F. J. Davis, "Improvements in the Threshold Detector Method of Fast Neutron Dosimetry," Health Phys. 1, 169 (1958).

7. Allen, L., Jr., W. A. Biggers, R. J. Prestwood, and R. K. Smith, "Cross Sections for the $S^{32}(n,p)P^{32}$ and the $S^{34}(n,\alpha)Si^{34}$ Reactions," Phys. Rev. 107, 1363 (1957).

8. Thorpe, M., Physics Division, Los Alamos Scientific Laboratory, unpublished data (September 1958).

9. Hurst, G. S., "A Fast Neutron Tissue Dosemeter," Brit. J. Radiol. 27, 353 (1954).

10. Wagner, E. B., and G. S. Hurst, "Advances in the Standard Proportional Counter Method of Fast Neutron Dosimetry," Rev. Sci. Instr. 29, 153 (1958).

11. Rossi, H. H., and G. Failla, "Tissue-Equivalent Ionization Chambers," Nucleonics 14, No. 2, 32 (1956).

12. Rosen, L., "Cross Sections Important to Reactor Design," Proceedings of the International Conference on Atomic Energy, Geneva, 1955, Vol. IV, pp. 97-104 (New York: United Nations, 1956).

13. Hurst, G. S., and R. Ritchie, Health Physics Division, Oak Ridge National Laboratory, personal communication (June 1958).